FACETS
a multidisciplinary open access science journal

RESEARCH ARTICLE

Quantifying the fate of wastewater nitrogen discharged to a Canadian river

Jason J. Venkiteswaran[a]*, Sherry L. Schiff[b], and Brian P. Ingalls[c]

[a]Department of Geography and Environmental Studies, Wilfrid Laurier University, 75 University Avenue West, Waterloo, ON N2L 3C5, Canada.; [b]Department of Earth and Environmental Sciences, University of Waterloo, 200 University Avenue West, Waterloo, ON N2L 3G1, Canada.; [c]Department of Applied Mathematics, University of Waterloo, 200 University Avenue West, Waterloo, ON N2L 3G1, Canada.

*jvenkiteswaran@wlu.ca

Abstract

Addition of nutrients, such as nitrogen, can degrade water quality in lakes, rivers, and estuaries. To predict the fate of nutrient inputs, an understanding of the biogeochemical cycling of nutrients is needed. We develop and employ a novel, parsimonious, process-based model of nitrogen concentrations and stable isotopes that quantifies the competing processes of volatilization, biological assimilation, nitrification, and denitrification in nutrient-impacted rivers. Calibration of the model to nitrogen discharges from two wastewater treatment plants in the Grand River, Ontario, Canada, show that ammonia volatilization was negligible relative to biological assimilation, nitrification, and denitrification within 5 km of the discharge points.

Key words: river, nitrogen, nitrate, ammonia, wastewater, isotope

OPEN ACCESS

Citation: Venkiteswaran JJ, Schiff SL, and Ingalls BP. 2019. Quantifying the fate of wastewater nitrogen discharged to a Canadian river. FACETS 4: 315–335. doi:10.1139/facets-2018-0028

Handling Editor: Tom A. Al

Received: July 30, 2018

Accepted: March 24, 2019

Published: July 22, 2019

Published by: Canadian Science Publishing

Introduction

Nitrogen (N) is essential for life but can be present in the environment in excess of growth requirements due to human activities. N is a common point-source pollutant to aquatic systems from wastewater treatment plants (WWTPs). Nitrate (NO_3^-) and total ammonia nitrogen (TAN; where TAN includes both ammonia (NH_3) and ammonium (NH_4^+)) are the two inorganic N forms that determine the critical loads beyond which aquatic ecosystems experience eutrophication or acidification (Posch et al. 2001; Schindler et al. 2006). The fate of these inorganic N species is a key determinant in the health of ecosystems and the services they provide to humans. TAN can be both a fertilizer of and detriment to aquatic life. At elevated concentrations, NH_3 is toxic to aquatic life (Canadian Council of Ministers of the Environment 2010). Similarly, elevated concentrations of NO_3^- degrade water quality by harming aquatic life (Canadian Council of Ministers of the Environment 2012), and those above drinking water limits can lead to adverse health effects in people (Iwanyshyn et al. 2008). Consequently, understanding the environmental fate of TAN and NO_3^- discharged to surface waters is important for managing of human-disturbed aquatic ecosystems.

Many processes remove N from aquatic ecosystems. By understanding the relative contributions of each process and the factors that affect their rates, the environmental fate of N loading to aquatic ecosystems can be predicted (Iwanyshyn et al. 2008). Successful nutrient mitigation strategies in larger aquatic ecosystems rely on using smaller, tractable ecosystems as realistic and replicatable systems (Schindler 1998; Dodds and Welch 2000; Withers and Lord 2002; Webster et al. 2003; Sharpley et al. 2009). The concept of nutrient spiralling in streams was developed to describe the cycling and

transport of nutrients in small lotic ecosystem (Newbold et al. 1981, 1982, 1983) and is based on downstream changes in nutrient concentrations. Nutrient spiralling techniques have been improved by adding ^{15}N-enriched compounds as a tracer and following them through different pools (e.g., Mulholland et al. 2000, 2004, 2008; Tank et al. 2000; Earl et al. 2006; Hall et al. 2009). In a similar fashion, low nutrient streams can be spiked with nutrients and changes in the nutrient pulse can be used to understand ecosystem metabolism of nutrients (e.g., Davis and Minshall 1999; Hall and Tank 2003). These studies are often restricted to short lengths of streams where the hydrology can be well characterized and to smaller systems in general. The understanding of nutrient spiralling in large impacted rivers is often confounded by a heterogeneous river morphology, frequent run-of-the-river dams, groundwater, and multiple nutrient inputs, and it consequently relies on the intensive work conducted in these smaller systems supplemented by sampling campaigns of both concentration and stable isotopes of N species. Further, observed values are a cumulative result of a plethora of contemporaneous N cycling processes with rates that change in relative importance with distance from inputs and time of day. Disentangling the relative rates of these processes in large rivers is greatly aided by the additional information supplied by stable isotopes and the development of numerical models (Denk et al. 2017).

Stable isotope studies in rivers have shown that (*i*) NH_4^+ is preferentially incorporated into the food web compared with NO_3^- and (*ii*) some TAN is lost to volatilization to the atmosphere whereas some is nitrified to NO_3^- (Loomer 2008; Murray 2008; Hood et al. 2014). Denitrification results in N attenuation in rivers but to a lesser extent in well-oxygenated rivers (Laursen and Seitzinger 2002, 2004; Rosamond et al. 2011, 2012). The rates of these processes change from day to night in response to the release of photosynthetic O_2 into the water (Venkiteswaran et al. 2007, 2015; Wassenaar et al. 2010). δ^{15}N values have been used to qualitatively identify anthropogenic N in coastal areas (Fourqurean et al. 1997; Fry et al. 2000; Savage and Elmgren 2004; Derse et al. 2007). Few studies have attempted to quantify the importance of these competing processes and their role in attenuation of WWTP TAN and NO_3^- in lotic systems though these processes set the baseline δ^{15}N (isotopic ratios are hereafter reported as δ values) values used for benthic invertebrate and fish studies (e.g., Hood et al. 2014; Loomer et al. 2014).

Novel technical developments in the analysis of stable isotopes have allowed for improved assessment of nitrogen cycling in rivers including the use of the differences in δ^{15}N-N_2O and δ^{18}O-N_2O produced by nitrification versus denitrification (Thuss et al. 2014). Similarly, ecosystem metabolism techniques have recently been improved by the use of diel δ^{18}O-O_2 and δ^{13}C-DIC modelling (Tobias et al. 2007; Venkiteswaran et al. 2007; Holtgrieve et al. 2010; Parker et al. 2010) leading to a greater understanding of nutrient dynamics (Fourqurean et al. 1997; Fry et al. 2000; Savage and Elmgren 2004; Murray 2008). The isotopic labelling of benthic biofilm by differing NH_4^+ and NO_3^- sources has recently been described (Hood et al. 2014; Loomer et al. 2014; Peipoch et al. 2014). Here, we build on these studies by developing and testing a model that uses changes in concentrations and natural abundance (that is, not isotopically labelled) stable isotopic ratios to quantify the contributions of the various nitrogen-removal pathways in nutrient-impacted rivers. We applied this model to quantify the fate of N from the WWTP effluent discharges in a river highly impacted by both agricultural and WWTP nutrients.

The objectives of this research are to (*i*) quantify changes in concentrations and δ^{15}N values of TAN and NO_3^- with distance downstream from WWTPs; (*ii*) develop a parsimonious process-based model for N cycling and the fate of WWTP N in rivers, and assess model performance with field measurements; and (*iii*) provide model-based estimates of the rates of nitrification, denitrification, NH_3 volatilization, and N assimilation in WWTP plumes in a river impacted by both WWTP and agricultural nutrient inputs.

Methods

Field site

The Grand River, Ontario, is the largest river discharging into the Canadian side of Lake Erie (**Fig. 1**). Almost 1 million people live in its watershed and more than half of those rely on the river for drinking water. There are 30 wastewater treatment plants of varying sizes in the watershed where agriculture is the dominant land use (80%). We have previously studied the N and O_2 cycling in the Grand River (Rosamond et al. 2011, 2012; Jamieson et al. 2013; Venkiteswaran et al. 2014, 2015). Here, we focus on two large WWTPs in the central part of the watershed that serve a combined population of about 230 000.

Ecosystems the size of the Grand River are not amenable to experimental isotope tracer additions but nevertheless afford us the opportunity to assess many of the processes resultant from the discharge of nitrogen-rich WWTP effluent. These processes include assimilation of NH_4^+ by primary producers, nitrification of NH_4^+ to NO_3^-, loss of NH_3 to the atmosphere via volatilization, denitrification of NO_3^-, and dilution of both NH_4^+ and NO_3^-. Rather than simply a point-source addition of nutrients to a pristine ecosystem, WWTP effluent in the Grand River increases nutrients in an already nutrient-rich system (Venkiteswaran et al. 2015).

The upstream Waterloo WWTP serves an urban population of approximately 120 000 and discharges a mix of NH_4^+ and NO_3^- via a pipe on the west side of the river. The plume hugs that bank of the river for several kilometres downstream. At baseflow, WWTP discharge accounts for 10%–25% of river flow along this reach. The downstream Kitchener WWTP serves about 205 000 and discharges mostly NH_4^+ via a diffuser in the middle of the river. The plume hugs the east bank of the river for several kilometres downstream before several large river bends result in lateral mixing. The river is about 50 m wide through the entire sampling area. Together, the WWTPs discharge about 900 tonnesN/year (**Table S1**).

In the study reach, the Grand River flows over the stony and sandy Catfish Creek till (Karrow 1974). This forms a substrate for the patchy growth dominated by the macroalga *Cladophora* spp. and macrophytes *Myriophyllum spicatum* and *Stuckenia pectinatus*. Their biomass (about 1 kg/m^2) is greater below both WWTPs than above (Hood 2012).

Water in the Grand River is hard with dissolved inorganic carbon (DIC) concentrations around 50 mgC/L. Municipal drinking water, from both the Grand River and groundwater, is similarly hard, averaging 50 mgC/L of DIC or alkalinity of 400 mg/L ($CaCO_3$ equivalent). The use of residential water softeners produces WWTP effluent high in Cl^- (Region of Waterloo 2011). River dissolved organic carbon (DOC) concentrations are typically 6–8 mgC/L. The river is shallow through the sampled section, with mean depth at baseflow around 0.5 m. Typical river discharge during the sampling periods through these reaches was 2–13 m^3/s (Canadian Water Survey, https://wateroffice.ec.gc.ca/). Sampling occurred during stable base-flow conditions.

Agricultural activity and some small WWTPs in the watershed result in high nutrient concentrations in the river prior to the two main WWTPs in this study. Upstream NO_3^- concentrations are elevated (3–4 mgN/L), whereas NH_4^+ concentrations are low (<0.1 mgN/L) and both total phosphorus and soluble reactive phosphorus are high (70 µg/L and 10 µg/L, respectively).

Below each of the two WWTPs, eight sampling points were established based on availability of access to the river (**Fig. 1**). For each WWTP, the first site was immediately downstream of the effluent discharge point. The second was 100 m downstream for the Waterloo WWTP and 200 m downstream for the Kitchener WWTP. The others were about every 800–1000 m further downstream for about

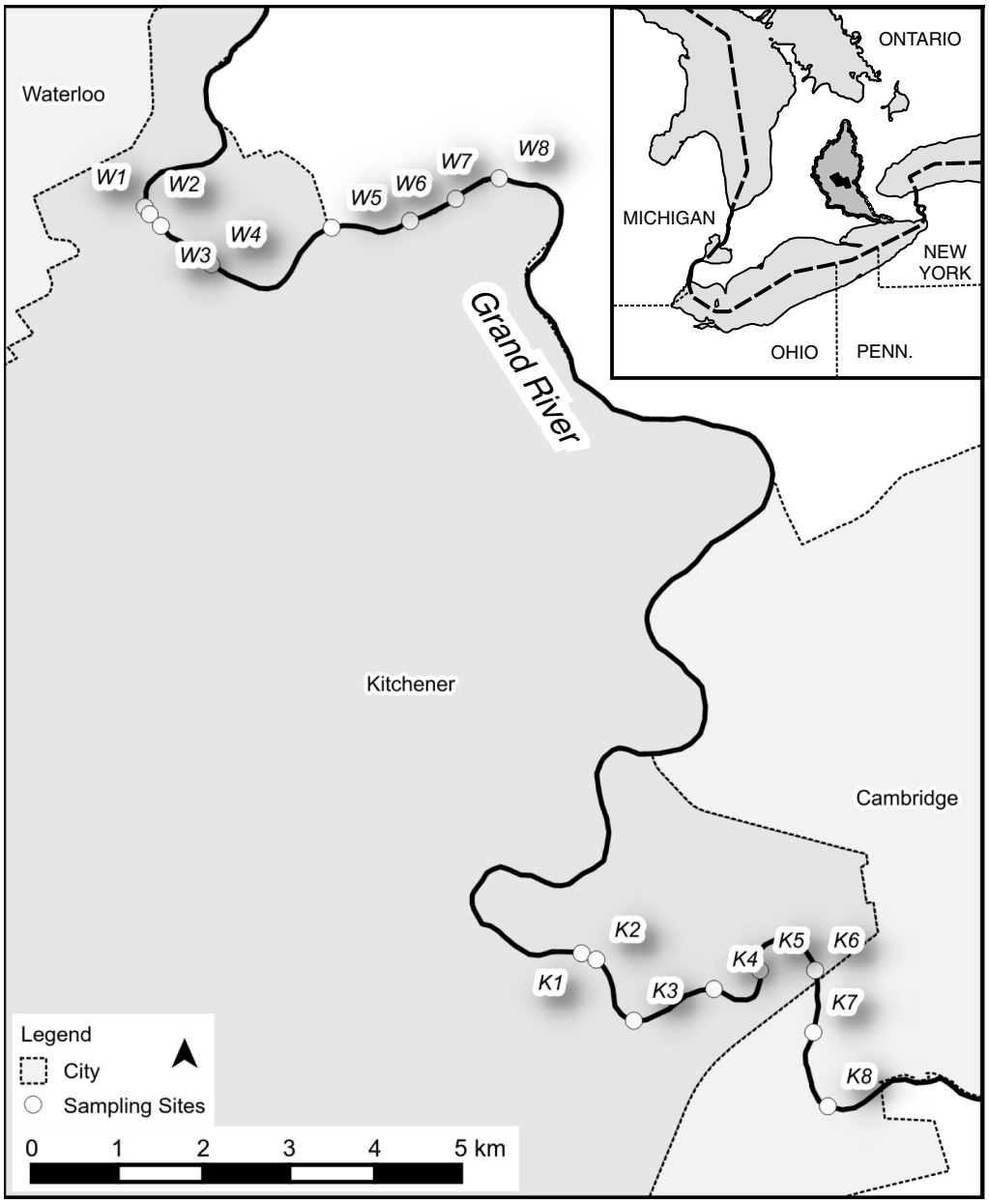

Fig. 1. Central portion of the Grand River watershed in southwestern Ontario, Canada. River flow is from north to south. Sampling sites below the Waterloo (W) and Kitchener (K) wastewater treatment plants are numbered 1–8. The cities of Cambridge, Kitchener, and Waterloo are highlighted as black blocks in the middle of the Grand River watershed in the inset map. Made with Natural Earth data (naturalearthdata.com) and information under licence with the Grand River Conservation Authority.

5 km (**Table S2**). At each site, samples for NH_4^+, NO_3^-, Cl^-, DOC, $\delta^{15}N\text{-}NH_4^+$, and $\delta^{15}N\text{-}NO_3^-$ were collected from the centre of the plume as identified by in situ measurement of conductivity (YSI 556 MPS). Samples were collected in high-density polyethylene bottles and immediately chilled in a cooler for transport to the laboratory, filtered to 0.45 µm, and kept cold (4 °C) until analyses. Samples for NH_4^+ and $\delta^{15}N\text{-}NH_4^+$ were immediately acidified to pH 4 with HCl and frozen until

analyses. In situ measurements of temperature and pH were made (YSI 556 MPS) with reported accuracy on pH and temperature of ±0.2 units and ±0.15 °C, respectively. To account for dilution of the effluent plume by river water, Cl^- at these elevated concentrations was assumed to be a conservative tracer and NH_4^+ and NO_3^- concentrations were adjusted accordingly.

WWTP plumes were sampled downstream of both sites twice. The plume from the Waterloo WWTP was sampled on 30 October 2007 (typical discharge 2–7 m^3/s) and 1 July 2008 (typical discharge 2–4 m^3/s). The plume from the Kitchener WWTP was sampled on 23 October 2007 (typical discharge 11–17 m^3/s) and 18 July 2008 (typical discharge 8–11 m^3/s).

Analyses

Anion concentrations were measured on a Dionex ICS-90 (Dionex, Sunnyvale, California) ion chromatograph. Precisions and detection limits of NO_3^- were 0.07 mgN/L (standard deviation of 15 replicates of a 5.0 mgN/L standard solution yielding 1.4% relative standard deviation) and 0.05 mgN/L, respectively. NO_2^- concentrations were rarely detectable. Precision of Cl^- measurements was <1 mg/L (standard deviations of 12 replicates of a 20 mg/L standard solution yielded 1.0% relative standard deviation). NH_4^+ concentrations were measured colorimetrically by the phenate colourimetric method EPA 350, (EPA 1993) on a Beckman DU500 (Beckman (Brea, California) UV/VIS spectrophotometer with a precision and detection limit of 0.005 mgN/L (0.5% relative standard deviation on a 1.0 mgN/L standard solution) and 0.015 mgN/L, respectively.

δ^{15}N-TAN was measured via the diffusion method on acidified discs (Zhang et al. 2007). Briefly, NH_4^+ is converted to NH_3 by increasing the sample pH; NH_3 is trapped in a filter pack containing a 1 cm GF/D filter, acidified with H_2SO_4 trapped in a polytetrafluoroethylene packet. The filter is dried and analysed for δ^{15}N on a Carlo Erba 1108 (Thermo, Waltham, Massachusetts) elemental analyzer (EA) coupled to a Micromass Isochrom isotope-ratio mass spectrometer (IRMS). Precision of δ^{15}N-NH_4^+ analysis was ±0.3‰. δ^{15}N-NO_3^- was measured via the $AgNO_3$ method. Briefly, sample volumes were reduced by evaporation, SO_4^{2-} was removed by barium precipitation, and NO_3^- was collected on anion exchange resin in a column. After being eluted from the column, AgO was added to precipitate $AgNO_3$, which was analyzed on the same EA-IRMS as above. Precision of δ^{15}N-NO_3^- was ±0.5‰. Methodological tests indicated that the $AgNO_3$ method can capture NO_2^- since NO_2^- oxidizes rapidly to NO_3^- even in filtered samples (Spoelstra 2004). Since previous measurements showed there was little NO_2^- in this river (NO_2^- was <5% of NO_3^-) the results presented here can be interpreted as δ^{15}N-NO_3^-.

Model setup

To interpret patterns in the data, a dynamic model (hereafter NANNO: nitrate, ammonia, nitrite, nitrous oxide) was developed to describe the dynamics of TAN, NO_2^-, NO_3^-, N_2O and their δ^{15}N values (eight states, in total). The model was implemented in R (R Core Team 2016) using the simecol (Petzoldt and Rinke 2007) package. Five processes were modelled: volatilization of NH_3, two-step nitrification ($NH_4^+ \rightarrow NO_2^-$ and $NO_2^- \rightarrow NO_3^-$), denitrification ($NO_3^- \rightarrow N_2O$), and biological assimilation of NH_4^+ (**Fig. 2**). We note that complete ammonia oxidation (comammox) by a single organism has recently been identified (van Kessel et al. 2015) and assume that any such contribution is negligible or encompassed by the model structure. In the model, N_2O produced by denitrification is allowed to accumulate rather than being further reduced to N_2; this choice was made because the N_2O:N_2 ratio produced during denitrification varies widely and once nitrogen is removed from the TAN and NO_3^- pools, it is very unlikely to return to those pools especially in a system where N is in excess. Similarly, the biological assimilation of NO_3^- was not included given that NH_4^+ is in excess. Metabolic costs suggest NH_4^+ is the preferred source of nitrogen over NO_3^- for phytoplankton and

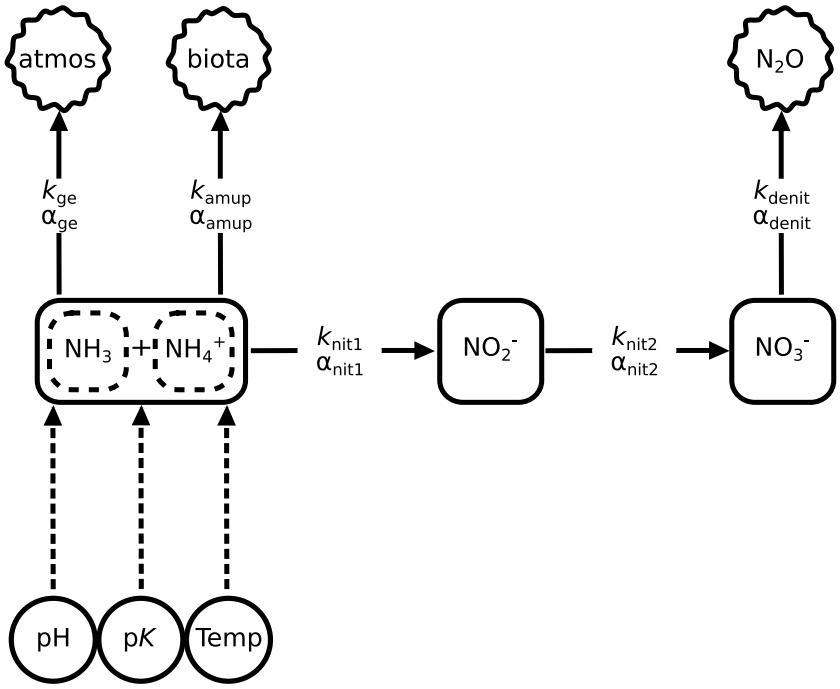

Fig. 2. Nitrogen pathways in the eight-state NANNO (nitrate, ammonia, nitrite, nitrous oxide) model. Each box represents a stock or pool. Circles represent data inputs to the model. Flows of nitrogen between stocks are identified with arrows, accompanied by first-order rate constants, *k*. Clouds indicate a loss of nitrogen from the system. Total ammonia nitrogen is modelled as ammonia (NH_3) and ammonium (NH_4^+). The ratio is set by measured temperature and pH, and calculated p*K* values. Ammonia gas exchange (ge) is modelled via the thin boundary layer model (Denmead and Freney 1992). Ammonium assimilation (amup) by biota is modelled as a loss of NH_4^+. Two-step nitrification (nit1, nit2) is modelled as NH_4^+ to NO_2^- to NO_3^-. Denitrification (denit) is modelled as a loss of NO_3^- to N_2O. Each stock is modelled independently for each isotope and flows are adjusted by isotope fractionation factors (α).

aquatic plants (Mariotti et al. 1982; Yoneyama et al. 1991; Collier et al. 2012) and that cycling of NH_4^+ is rapid (Mulholland et al. 2000). Isotopic evidence suggests this is also true for macrophytes in the Grand River (Hood 2012; Hood et al. 2014). Each process is associated with isotopic fractionation (ε, where $\varepsilon = \alpha - 1$ and $\alpha = R_{product}/R_{reactant}$). Fractionation factors for physical processes are typically known with greater precision than biological ones. Since the Grand River is very well buffered, average measured pH values were used for TAN speciation calculations. Model parameters and commonly reported values are summarized in **Table 1**.

To simplify modelling efforts, the common time-for-distance substitution was made, using Cl^- as a conservative tracer, and NH_4^+ and NO_3^- concentrations were adjusted accordingly. Additionally, to avoid requiring river surface area for gas exchange with the atmosphere, all rate constants, including the gas exchange coefficient, were modelled with units of per time. First-order rate kinetics were used for nitrification (Dinçer and Kargı 2000; Chen et al. 2006), biological NH_4^+ assimilation (MacIsaac and Dugdale 1969; D'Elia and DeBoer 1978), and denitrification (Dinçer and Kargı 2000). Sensitivity of model outputs to these parameters is described in **Supplementary Material 1**. NH_3 gas exchange was modelled with the thin-boundary layer equation (Denmead and Freney 1992) assuming the atmospheric NH_3 concentration was negligible (ppb-range concentration (Finlayson-Pitts and Pitts 1986; Mészáros 1992)). Ranges of potential gas exchange coefficients can be estimated from river

Table 1. Parameters and typical values used in modelling wastewater treatment plant plumes in the Grand River, Ontario via NANNO (nitrate, ammonia, nitrite, nitrous oxide).

Parameter	Description	Typical value or range	Units	Reference
k_{ge}	Gas exchange coefficient	0.0001–0.0006	t^{-1}, m^{-1}	Jamieson et al. 2013; Venkiteswaran et al. 2015
k_{nit1}	Nitrification rate constant: NH_4^+ to NO_2^-	0–0.01	t^{-1}, m^{-1}	—
k_{nit2}	Nitrification rate constant: NO_2^- to NO_3^-	0–0.01	t^{-1}, m^{-1}	—
k_{denit}	Denitrification rate constant	0–0.001	t^{-1}, m^{-1}	—
k_{amup}	Ammonium uptake rate constant	0–0.01	t^{-1}, m^{-1}	—
α_{NH3NH4}	Equilibrium isotope fractionation factor between NH_3 and NH_4^+	1.047	Unitless	Hermes et al. 1985; Li et al. 2012
α_{ge}	Kinetic isotope fractionation factor for gas exchange of NH_3	0.995–1.000	Unitless	Thode et al. 1945; Kirshenbaum et al. 1947; Norlin et al. 2002
α_{nit1}	Isotope fractionation factor for nitrification: NH_4^+ to NO_2^-	0.990–1.000	Unitless	Gammons et al. 2010
α_{nit2}	Isotope fractionation factor for nitrification: NO_2^- to NO_3^-	0.990–1.000	Unitless	Gammons et al. 2010
α_{denit}	Isotope fractionation factor for denitrification: NO_3^- to N_2O	0.985–1.000	Unitless	Sebilo et al. 2003
α_{amup}	Isotope fractionation for NH_4^+ uptake	0.973–1.000	Unitless	Delwiche and Steyn 1970; Mariotti et al. 1981; Hoch et al. 1992; Fogel and Cifuentes 1993
pH	Ph	7.5–8.5	Unitless	Measured in situ
Temp	Temperature	10–20	°C	Measured in situ
pK_a	Acid dissociation constant for NH_4^+	9.4	Unitless	Calculated (Olofsson 1975)

Note: Ranges were provided as constraints within which the model's fitting routine could search for possible values.

channel geometry (Raymond et al. 2012) and converted for use with NH_3 via Schmidt number scaling (Jähne et al. 1987), for example, at 20 °C the Schmidt number for NH_3 in freshwater is 585 (Kreith 2000).

For the Grand River, the gas exchange coefficient for O_2 (0.1–0.5 m/h) has been estimated for its length with focus on the areas including the WWTPs (Jamieson et al. 2013; Venkiteswaran et al. 2015). These values were converted for use with NH_3 recognizing that because of differences in solubility between NH_3 and O_2 the air-side and water-side resistances are very different (Blomquist et al. 2006; Johnson 2010). Measured river depths at all sampling sites were 0.5–1.0 m. River velocities are measured at several sites by the Water Survey of Canada and modelled at other locations by the Grand River Conservation Authority (Veale and Cooke 2016). Modelled river velocities were 0.2–0.4 m/s for typical flow conditions (M.J. Anderson, personal communication, 2015). Gas exchange coefficients were converted from units of vertical distance per time to units of per distance by dividing by river depth and multiplying by river velocity. This produces a range of k_{ge} values for NH_3 of 0.0001–0.0006 m^{-1} downstream of the WWTPs.

An initial best-fit solution for each set of field data was found by allowing the model to find a combination of rate constants (≥0), isotopic fractionation factors (between the lowest literature α values (i.e., the strongest values) and 1), and initial values that minimized the sum of squared errors between field data and model output.

Results

Field measures of N concentrations and isotopes in WWTP plumes

Waterloo

On both dates, TAN concentrations declined from 5–7 mgN/L to ≪1 mgN/L by the 5 km sampling point, although the rate of decline was much faster on 1 July 2008 than on 30 October 2007. Nitrate response in the plumes was different on both dates: on 30 October 2007, there was a gradual decline in NO_3^- but on 1 July 2008 there was an increase of >1 mgN/L. Together, these results suggest different fates for N in the Waterloo plume on each date.

On 30 October 2007, δ^{15}N-TAN values increase rapidly from 12‰ to 30‰ in the first 500 m before concentrations became too low for analyses. On 1 July 2008, only the initial sample had an adequate TAN concentration for δ^{15}N-TAN analysis but TAN persisted at a greater distance downstream than on 30 October 2007. On both dates, the δ^{15}N-NO_3^- values declined from 16‰ to 11‰ within the first 1 km, and then rose gradually.

Kitchener

TAN concentrations downstream of the Kitchener WWTP declined to <1 mgN/L over the 5.5 km sampling transect from initial values of 14 mgN/L and 4 mgN/L on 23 October 2007 and 18 July 2008. Nitrate concentrations increased substantially on 23 October 2007, from 0.8 mgN/L to 5.9 mgN/L, and to a lesser degree on 18 July 2008 from 1.3 mgN/L to 3.1 mgN/L.

δ^{15}N-TAN values increased on both days, by 22‰ on 23 October 2007 and by 12‰ on 18 July 2008 over the 5.5 km. Unlike at Waterloo, the δ^{15}N-NO_3^- values changed only by around 3‰; decreasing on 23 October 2007 and increasing on 18 July 2008.

Model development: effect of N cycling processes on coupled N concentrations and isotopes

The coupling of concentrations and isotopes in a simple process-based model shows that the various N cycling processes result in different patterns at the river scale. These results suggest the model may reproduce the variety of expected patterns from each process in the model. Additionally, as we describe next, the dynamic features of each process are sufficiently distinct that we would expect the model to be identifiable. That is, we would expect to arrive at a tight estimate of the kinetic parameters given a sufficiently rich field data set. If this were not the case, then there would be less likelihood that a unique model solution describing TAN, NO_2^-, NO_3^-, N_2O and their δ^{15}N values could be found.

We could include many processes or only a few but the field data inform us as to what processes we must include because the isotopic effects are very different for the different processes. Both NH_3 degassing and biological NH_4^+ assimilation result in expected and rapid increases in δ^{15}N values, but increases in δ^{15}N-TAN have different values with similar decreased in TAN because of the difference in isotopic fractionation between the two processes. Nitrification alone produces a transient but small increase in NO_2^- (<20% of DIN (dissolved inorganic nitrogen, DIN = TAN + NO_3^-) at its greatest) as NH_4^+ is oxidized to NO_3^-. There is a characteristic initial dip in δ^{15}N-NO_3^- that must be a function of the initial δ^{15}N values and isotopic fractionation (α_{nit1} and α_{nit2}) and may be exploitable as an identifier of significant nitrification. Denitrification alone, unlikely in a WWTP plume in a shallow oxygenated river during the day, results in a clear decline in NO_3^- associated with an increase in δ^{15}N-NO_3^- and no changes in TAN or δ^{15}N-TAN. The model predicts a corresponding increase in N_2O and a transient dip in δ^{15}N-N_2O values that depends on initial conditions and the strength of α_{denit}.

An initial structural identifiability analysis (Bellman and Åström 1970) (see **Supplementary Material 1**) of the model dynamics and outputs confirmed that with the available data, it would not be possible to separately estimate the rates at which the equilibrated TAN pool (NH_3 and NH_4^+) is lost through gas exchange and biological NH_4^+ assimilation processes. This conclusion is valid regardless of the quality of the concentration data and $\delta^{15}N$ values (see also **Supplementary Material 1**). However, the gas exchange coefficient can be independently quantified.

Consequently, we simplified the model by fixing from independent sources the gas exchange coefficient as quantified in these areas of the Grand River (k_{ge} (Jamieson et al. 2013; Venkiteswaran et al. 2015)) and its isotope fractionation factor as quantified in laboratory experiments (α_{ge} (Thode et al. 1945; Kirshenbaum et al. 1947; Norlin et al. 2002).

We fit the resulting model separately to the four field data sets and then, in each case, applied uncertainty analysis as described in Methods. The results varied, but from this preliminary analysis (results not shown) we discovered that in every case the available data were not sufficient to provide accurate estimates of the eight free parameters. In particular, the k_{nit2} and α_{nit2} parameters could not be well-estimated from any of the data sets. Consequently, we reduced the model further, by removing NO_2^- and instead describe a single-step nitrification process (k_{nit1} and α_{nit1}) where NH_4^+ is oxidized to NO_3^-; this is justified given that NO_2^- concentrations are low compared with NO_3^- and TAN and not accumulating. The resulting system has six states: TAN, NO_3^-, N_2O, $\delta^{15}N$-TAN, $\delta^{15}N$-NO_3^-, and $\delta^{15}N$-N_2O. Results of fitting and uncertainty analysis, as described in Methods, are shown in **Tables S3**–**S6**.

In the case of the Kitchener 2007 data set (**Table S6**), the k parameters for nitrification and denitrification all appear to be reasonably well constrained. The α estimates are less confident. Two of the best-fit α value estimates, α_{dnit} and α_{amup}, are at the bounds of the range of α allowed (**Table 1**; (0.975, 1)), suggesting the data provide minimal useful information about their values. Moreover, while two of the sensitivities are not unreasonably low, the confidence intervals are considerably larger than the search space, which has a width of only 2.5% (25‰).

For the Kitchener 2008 best fit, the trend in certainty is similar but the data constrain the parameter estimates to a lower degree. Data from Waterloo (2007 and 2008, **Tables S4** and **S5**) provide even less ability to constrain the rates likely because the system behaviour is not as dynamic, i.e., the range in $\delta^{15}N$ values is small despite the change in concentration being large.

Discussion

The process-based NANNO model was able to reproduce the observed dynamics in concentrations and the $\delta^{15}N$ values of TAN and NO_3^- (**Tables S3**–**S6**). Results from two seasons, with different proportional fates of N processing, at two different WWTPs with different TAN:NO_3^- ratios in their effluent indicate a good degree of coherence between model results and field data (**Figs. 3**–**6** and **Tables S3**–**S6**). Additionally, the shapes of the curves (increases, decreases, and plateaus) were all generally reproducible by the model. The model was least successful in reproducing behaviour when there were increases in NO_3^- concentration without a change in $\delta^{15}N$-NO_3^-. This scenario suggests nitrification where the new NO_3^- has the same $\delta^{15}N$-NO_3^- as the extant NO_3^-.

Although process-based models provide several advantages over purely empirical ones, the goodness of fit and performance of such models depends on their particular application (Saloranta et al. 2003). The variables in this underdetermined model system were constrained in several ways. The variables in this underdetermined model system were constrained in several ways, but the available data were insufficient to identify a unique best-fit model parameterization within the constrained parameter

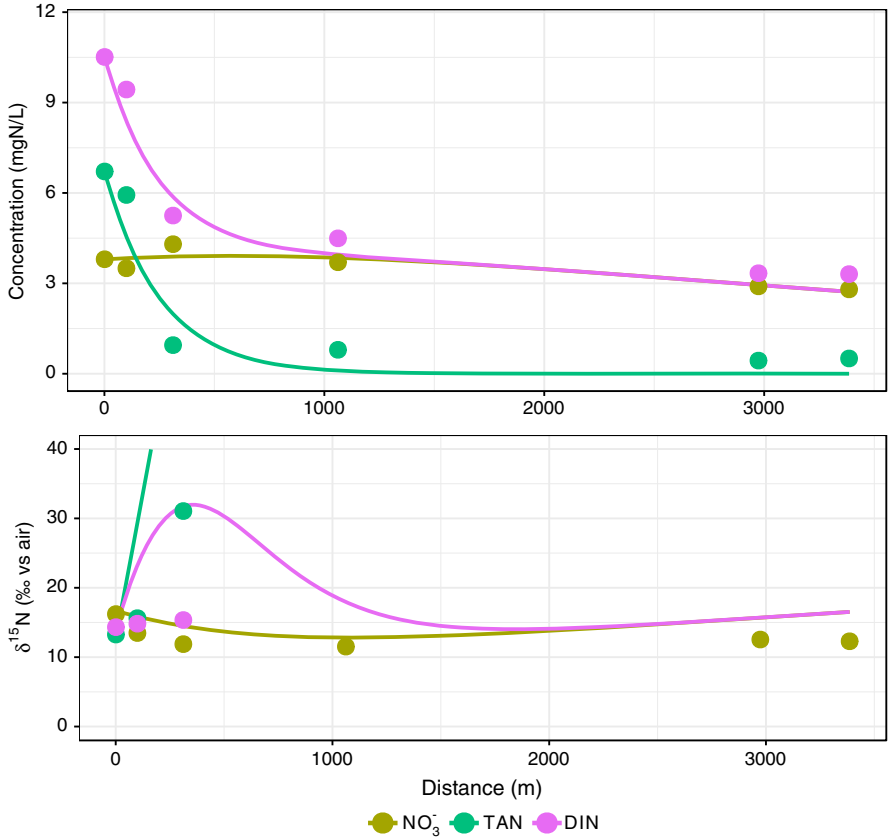

Fig. 3. Waterloo wastewater treatment plants (WWTP) plumes on 30 October 2007. Measured field data (adjusted for WWTP plume dilution using Cl^- data) are shown as points. Best-fit model results are shown as curves. Parameters used in the model are given in **Table 1**. Dissolved inorganic nitrogen (DIN = TAN + NO_3^- and mass-weighted δ^{15}N-DIN) is also plotted to show where there is N loss from the system either through degassing, assimilation or denitrification.

space. The local sensitivity of specific behaviours on the resulting modelling parameters can only be confidently assessed once best-fit model solutions have been developed (Moore and Doherty 2005). This issue is typical of ecosystem models, which nevertheless are often used to predict the fate of nitrogen, oxygen, and biological oxygen demand in rivers (e.g., the Grand River Simulation Model that is used by the local Grand River Conservation Authority when making decisions about nutrient loads and river health).

In all four cases, N is lost from the river downstream of the WWTPs. Rates for each N process can be summarized by their rate constants (**Tables S3–S6**) but are better compared as the mass of N transformed by each process (**Table 2**). In three of four cases, NH_3 loss via volatilization was much lower than NH_4^+ loss via update or nitrification (**Table 2**) (Chen 2013; Jamieson et al. 2013; Chen et al. 2014; Venkiteswaran et al. 2015). Thus N from WWTP effluent largely remained in and was transformed with the Grand River in these three cases where river pH values were 7.6–8.4, well below the pK_a value of 9.4, and with high rates of community metabolism (Chen 2013; Jamieson et al. 2013; Chen et al. 2014; Venkiteswaran et al. 2015).

In both Waterloo cases, denitrification played a modest role in reducing N concentrations (**Table 2**). N_2O concentrations in and fluxes from the Grand River are high downstream of these WWTPs

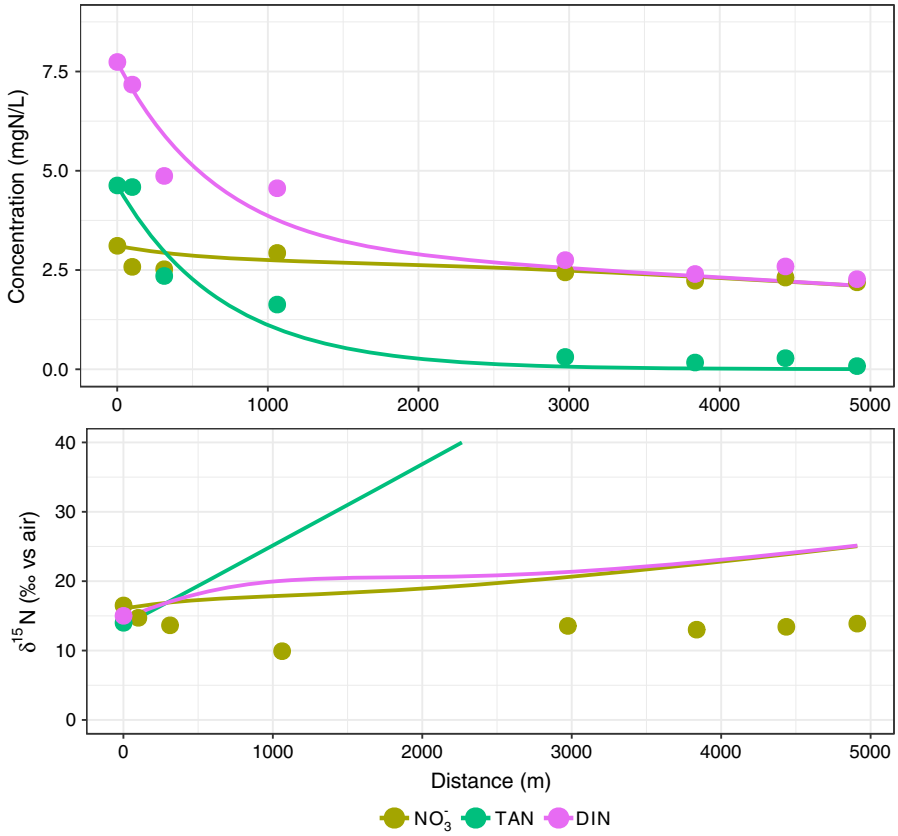

Fig. 4. Waterloo wastewater treatment plants plumes on 1 July 2008. Measured field data are shown as points. Best-fit model results are shown as curves. Parameters used in the model are given in **Table 1**. Dissolved inorganic nitrogen (DIN = TAN + NO_3^- and mass-weighted δ^{15}N-DIN) is plotted to show where there is nitrogen loss from the system either through degassing, assimilation or denitrification.

(Rosamond et al. 2011, 2012; Venkiteswaran et al. 2014). More detailed sampling of N_2O and its δ^{15}N values may provide additional constraints to improve the model fit.

Nitrification played a moderate role in N cycling in all four cases. There were no clear correlations between nitrification rates and rates of other N processes suggesting that predictions about the fate of N in the Grand River cannot be simply derived from other components of ecosystem metabolism. Where measurable, NO_2^- concentrations and δ^{15}N values may provide additional information to the model by constraining nitrification.

The δ^{15}N values of benthic periphyton and invertebrates (Loomer 2008; Loomer et al. 2014) as well as macrophtes (Hood 2012; Hood et al. 2014) are often used as indicators of different N sources and N pollution because they form the base of the food web. Interpreting these data requires an ability to understand and predict the fate of large isotopically distinct N sources like WWTP effluent since the δ^{15}N values measured in biota ultimately depend on the source of N and isotopic fractionation during biological assimilation. Moreover, macrophytes integrate N over a much longer time scale than the effluent-plume travel time or diel variability (Hood et al. 2014; Loomer et al. 2014).

There are several key model parameters that are insufficiently characterized, such as isotopic fractionation during biological assimilation of both TAN and NO_3^-, preferential use of different

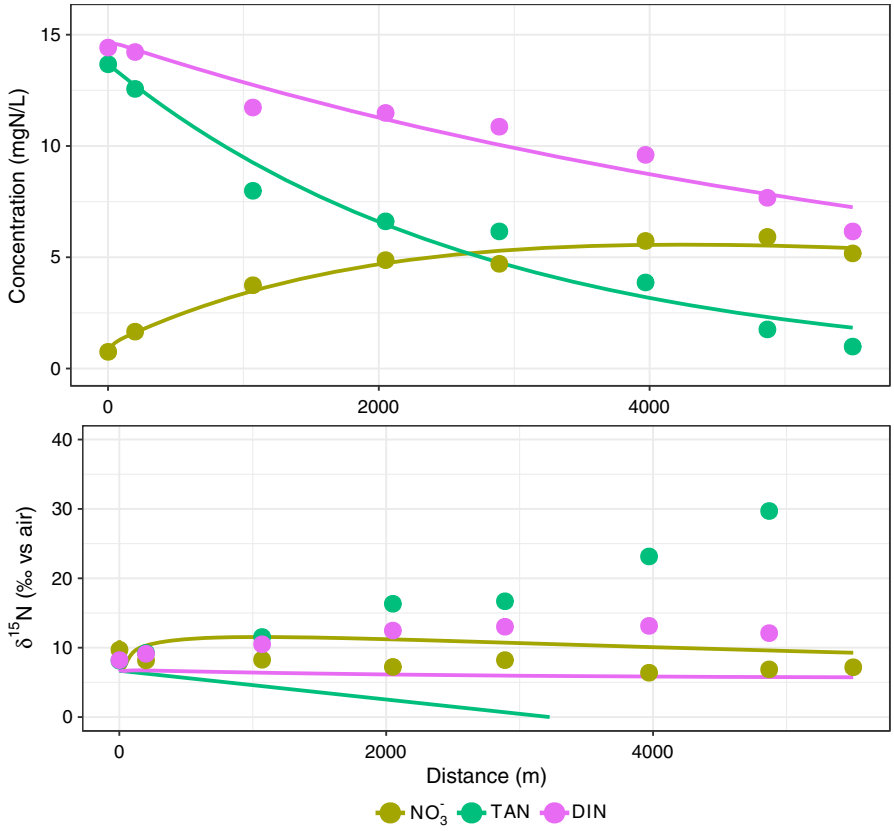

Fig. 5. Kitchener wastewater treatment plants plumes on 23 October 2007. Measured field data are shown as points. Best-fit model results are shown as curves. Parameters used in the model are given in **Table 1**. Dissolved inorganic nitrogen (DIN = TAN + NO_3^- and mass-weighted δ^{15}N-DIN) is plotted to show where there is nitrogen loss from the system either through degassing, assimilation or denitrification.

N species, and release of TAN and NO_3^-. The variability in isotopic fractionation during biological NH_4^+ assimilation is large and varies nonlinearly with concentration (Hoch et al. 1992; Pennock et al. 1996; Yoneyama et al. 2001). This poses a vexing problem at the ecosystem scale since the isotopic enrichment—concentration relationship varies between species and both concentrations and species vary within ecosystems.

The mass and δ^{15}N of river biomass are difficult to capture in the parsimonious NANNO model structure; model fitting may be improved if the release of TAN and NO_3^- by biomass contributes significantly to river N relative to WWTP effluent (Loomer et al. 2014). Nitrogen assimilation and release rates can be estimated with nutrient spiralling techniques but this analysis often conflates TAN and NO_3^-. It is therefore difficult to discern which N form is used, which is released, and how these results apply to a river with more than 100 km of upstream nutrient inputs. The degree of importance, if any, to dissolved organic N mineralization or N release from microbes and macrophytes in the nutrient-replete WWTP plumes is unknown.

Understanding the ecosystem effects of changes in nitrogen sources, such as altering WWTPs to produce only NO_3^- instead of NH_4^+ to improve river O_2 concentrations requires knowledge about which N enters the base of the foodweb via primary producers and consumers. In cases where δ^{15}N-NO_3^- and δ^{15}N-TAN values are far enough apart, or one is changing while the other is constant, the use of each by

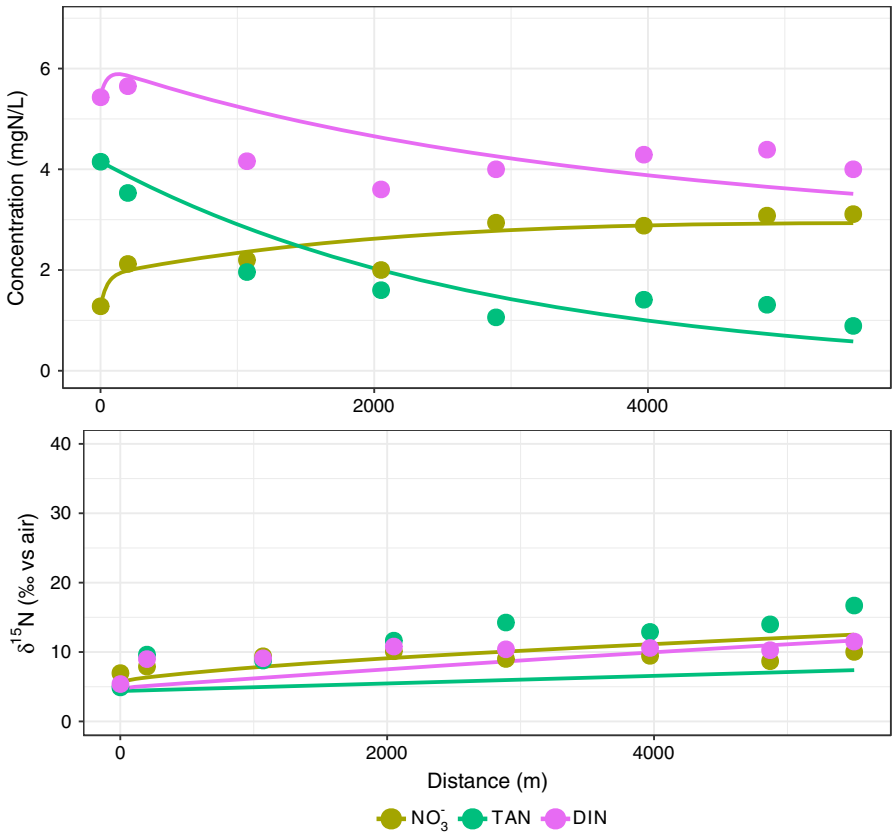

Fig. 6. Kitchener wastewater treatment plants plumes on 18 July 2008. Measured field data are shown as points. Best-fit model results are shown as curves. Parameters used in the model are given in Table 1. Dissolved inorganic nitrogen (DIN = TAN + NO_3^- and mass-weighted δ^{15}N-DIN) is plotted to show where there is nitrogen loss from the system either through degassing, assimilation or denitrification.

Table 2. Summary of all rates from best fits.

	Waterloo WWTP 2007-10-30	Waterloo WWTP 2008-07-01	Kitchener WWTP 2007-10-23	Kitchener WWTP 2008-07-18
NH_3 Volatilization	2.3	0.11	0.02	0.12
NH_4^+ uptake	0.16	0.37	5.0	1.9
Nitrification	2.1	7.3	8.4	3.0
Denitrification	3.0	4.1	0.30	0.41

Note: Reported as X mgN/L or mass of N transformed by each process in the river reaches under study. WWTP, wastewater treatment plant.

primary producers and consumers may be teased apart. Biological NO_3^- assimilation is associated with little to no isotopic fractionation (Mariotti et al. 1981; Yoneyama et al. 1998, 2001) and in the WWTPs' effluent plumes in the Grand River δ^{15}N-NO_3^- values do not vary as much as δ^{15}N-TAN values. In such scenarios, response to increasing δ^{15}N-TAN may be observable as a concomitant increase in the δ^{15}N of primary producers and consumers (Hood et al. 2014; Loomer et al. 2014).

Since O_2, N, and phosphorus cycles are strongly linked, improving the understanding of nitrogen processes allows previous work on O_2 and phosphorus cycling in the Grand River (Barlow-Busch et al. 2006; Venkiteswaran et al. 2014, 2015) to be extended to process-based biogeochemical models that incorporate multiple elements and their isotopes. Components that may be added to NANNO to improve constraints on nitrogen processes include $\delta^{18}O\text{-}NO_3^-$ values. However, recent work has demonstrated that predicting the $\delta^{18}O$ values of nitrogenous species is more complicated than originally thought because there are poorly understood abiotic factors that alter the $\delta^{18}O$ value of NO_2^- and NO_3^- as well as multiple pathways to produce N_2O (Buchwald and Casciotti 2010; Casciotti et al. 2010; Snider et al. 2010, 2012, 2013, 2015; Buchwald et al. 2012). Nevertheless, there are opportunities to produce a more constrainable model.

Conclusions

We have presented a process-based isotopic model of key nitrogen species for use in nutrient plumes in rivers. The NANNO model successfully reproduced observed dynamics in TAN and NO_3^- concentrations and their $\delta^{15}N$ values including seasonal differences in the way N species were processed. The ability to model these processes is a key step to making predictions about how improvements in WWTP effluent will affect receiving waters.

Acknowledgements

Canada's Natural Science and Engineering Research Council funded the field research under STPGP 336807-06 and STPGP 381058-09. Grand River Conservation Authority provided assistance with field data. A portion of this was work performed while under the sponsorship of the International Atomic Energy Agency Coordinated Research Project F32007. Field and laboratory assistance was provided by Richard Elgood, Neus Otero, Marilla Murray, Sarah Sine, David Snider, and Madeline Rosamond. We thank Thomas Petzoldt for the ease with which the simecol package can be used and Hadley Wickham and Winston Chang for their work on and documentation of ggplot2. Data and code are available as part of the NANNO package at doi:10.5281/zenodo.2647564.

Author contributions

JJV and SLS conceived and designed the study. JJV and SLS performed the experiments/collected the data. JJV, SLS, and BPI analyzed and interpreted the data. JJV, SLS, and BPI contributed resources. JJV, SLS, and BPI drafted or revised the manuscript.

Competing interests

The authors have declared that no competing interests exist.

Data availability statement

All relevant data are within the paper and in the Supplementary Material. Data and code are available as part of the NANNO package at DOI: 10.5281/zenodo.2647564.

Supplementary material

The following Supplementary Material is available with the article through the journal website at doi:10.1139/facets-2018-0028.

Supplementary Material 1

References

Barlow-Busch L, Baulch HM, and Taylor WD. 2006. Phosphate uptake by seston and epilithon in the Grand River, southern Ontario. Aquatic Sciences, 68(2): 181–192. DOI: 10.1007/s00027-006-0806-9

Bellman R, and Åström KJ. 1970. On structural identifiability. Mathematical Biosciences, 7(3–4): 329–339. DOI: 10.1016/0025-5564(70)90132-X

Blomquist BW, Fairall CW, Huebert BJ, Kieber DJ, and Westby GR. 2006. DMS sea-air transfer velocity: direct measurements by eddy covariance and parameterization based on the NOAA/COARE gas transfer model. Geophysical Research Letters, 33(7): L07601. DOI: 10.1029/2006GL025735

Buchwald C, and Casciotti KL. 2010. Oxygen isotopic fractionation and exchange during bacterial nitrite oxidation. Limnology and Oceanography, 55(3): 1064–1074. DOI: 10.4319/lo.2010.55.3.1064

Buchwald C, Santoro AE, McIlvin MR, and Casciotti KL. 2012. Oxygen isotopic composition of nitrate and nitrite produced by nitrifying cocultures and natural marine assemblages. Limnology and Oceanography, 57(5): 1361–1375. DOI: 10.4319/lo.2012.57.5.1361

Canadian Council of Ministers of the Environment. 2010. Canadian water quality guidelines for the protection of aquatic life: ammonia. *In* Canadian environmental quality guidelines. Canadian Council of Ministers of the Environment, Winnipeg, Manitoba. pp. 1–8 [online]: Available from ceqg-rcqe.ccme.ca/download/en/141/.

Canadian Council of Ministers of the Environment. 2012. Canadian water quality guidelines for the protection of aquatic life: nitrate ion. *In* Canadian environmental quality guidelines. Canadian Council of Ministers of the Environment, Winnipeg, Manitoba. pp. 1–17 [online]: Available from ceqg-rcqe.ccme.ca/download/en/197/.

Casciotti KL, McIlvin M, and Buchwald C. 2010. Oxygen isotopic exchange and fractionation during bacterial ammonia oxidation. Limnology and Oceanography, 55(2): 753–762. DOI: 10.4319/lo.2010.55.2.0753

Chen G. 2013. Ecosystem oxygen metabolism in an impacted temperate river network: application of the δ^{18}O-DO approach. Ph.D. thesis, University of Waterloo, Waterloo, Ontario [online]: Available from hdl.handle.net/10012/7412.

Chen G, Venkiteswaran JJ, Schiff SL, and Taylor WD. 2014. Inverse modeling of dissolved O_2 and δ^{18}O-DO to estimate aquatic metabolism, reaeration and respiration isotopic fractionation: effects of variable light regimes and input uncertainties. Aquatic Sciences, 76(3): 313–329. DOI: 10.1007/s00027-014-0337-8

Chen S, Ling J, and Blancheton J-P. 2006. Nitrification kinetics of biofilm as affected by water quality factors. Aquacultural Engineering, 34(3): 179–197. DOI: 10.1016/j.aquaeng.2005.09.004

Collier JL, Lovindeer R, Xi Y, Radway JC, and Armstrong RA. 2012. Differences in growth and physiology of marine *Synechococcus* (cyanobacteria) on nitrate versus ammonium are not determined solely by nitrogen source redox state. Journal of Phycology, 48(1): 106–116. PMID: 27009655 DOI: 10.1111/j.1529-8817.2011.01100.x

Davis CJ, and Minshall WG. 1999. Nitrogen and phosphorus uptake in two Idaho (USA) headwater wilderness streams. Oecologia, 119(2): 247–255. PMID: 28307975 DOI: 10.1007/s004420050783

D'Elia CF, and DeBoer JA. 1978. Nutritional studies of two red algae. II. Kinetics of ammonium and nitrate uptake. Journal of Phycology, 14(3): 266–272. DOI: 10.1111/j.1529-8817.1978.tb00297.x

Delwiche CC, and Steyn PL. 1970. Nitrogen isotope fractionation in soils and microbial reactions. Environmental Science and Technology, 4(11): 929–935. DOI: 10.1021/es60046a004

Denk TRA, Mohn J, Decock C, Lewicka-Szczebak D, Harris E, Butterbach-Bahl K, et al. 2017. The nitrogen cycle: A review of isotope effects and isotope modeling approaches. Soil Biology and Biochemistry, 105: 121–137. DOI: 10.1016/j.soilbio.2016.11.015

Denmead OT, and Freney JR. 1992. Transfer coefficients for water-air exchange of ammonia, carbon dioxide and methane. Ecological Bulletins, 42: 31–41. DOI: 10.2307/20113103

Derse E, Knee KL, Wankel SD, Kendall C, Berg CJ, and Paytan A. 2007. Identifying sources of nitrogen to Hanalei Bay, Kauai, utilizing the nitrogen isotope signature of macroalgae. Environmental Science and Technology, 41(15): 5217–5223. PMID: 17822082 DOI: 10.1021/es0700449

Dinçer AR, and Kargı F. 2000. Kinetics of sequential nitrification and denitrification processes. Enzyme and Microbial Technology, 27(1–2): 37–42. PMID: 11118590 DOI: 10.1016/S0141-0229(00)00145-9

Dodds WKK, and Welch EB. 2000. Establishing nutrient criteria in streams. Journal of the North American Benthological Society, 19(1): 186–196. DOI: 10.2307/1468291

Earl SR, Valett HM, and Webster JR. 2006. Nitrogen saturation in stream ecosystems. Ecology, 87(12): 3140–3151. PMID: 17249238 DOI: 10.1890/0012-9658(2006)87[3140:NSISE]2.0.CO;2

EPA. 1993. Method 350.1: determination of ammonia nitrogen by semi-automated colorimetry. Revision 2.0 [online]: Available from epa.gov/sites/production/files/2015-06/documents/epa-350.1.pdf.

Finlayson-Pitts BJ, and Pitts JN Jr. 1986. Atmospheric chemistry: fundamentals and experimental techniques. John Wiley and Sons, New York, New York.

Fogel ML, and Cifuentes LA. 1993. Isotope fractionation during primary production. *In* Organic geochemistry. *Edited by* H.M. Engel and S.A. Macko Plenum Press, New York, New York. pp. 73–98.

Fourqurean J, Moore T, Fry B, and Hollibaugh J. 1997. Spatial and temporal variation in C:N:P ratios, $\delta^{15}N$, and $\delta^{13}C$ of eelgrass *Zostera marina* as indicators of ecosystem processes, Tomales Bay, California, USA. Marine Ecology Progress Series, 157: 147–157. DOI: 10.3354/meps157147

Fry B, Bern AL, Ross MS, and Meeder JF. 2000. $\delta^{15}N$ studies of nitrogen use by the red mangrove, *Rhizophora mangle* L. in South Florida. Estuarine, Coastal and Shelf Science, 50(2): 291–296. DOI: 10.1006/ecss.1999.0558

Gammons CH, Babcock JN, Parker SR, and Poulson SR. 2010. Diel cycling and stable isotopes of dissolved oxygen, dissolved inorganic carbon, and nitrogenous species in a stream receiving treated municipal sewage. Chemical Geology, 283: 44–55. DOI: 10.1016/j.chemgeo.2010.07.006

Hall RJO, and Tank JL. 2003. Ecosystem metabolism controls nitrogen uptake in streams in Grand Teton National Park, Wyoming. Limnology and Oceanography, 48(3): 1120–1128. DOI: 10.4319/lo.2003.48.3.1120

Hall RO, Tank JL, Sobota DJ, Mulholland PJ, O'Brien JM, Dodds WK, et al. 2009. Nitrate removal in stream ecosystems measured by ^{15}N addition experiments: total uptake. Limnology and Oceanography, 54(3): 653–665. DOI: 10.4319/lo.2009.54.3.0653

Hermes JD, Weiss PM, and Cleland WW. 1985. Use of nitrogen-15 and deuterium isotope effects to determine the chemical mechanism of phenylalanine ammonia-lyase. Biochemistry, 24(12): 2959–2967. PMID: 3893533 DOI: 10.1021/bi00333a023

Hoch MP, Fogel ML, and Kirchman DL. 1992. Isotope fractionation associated with ammonium uptake by a marine bacterium. Limnology and Oceanography, 37(7): 1447–1459. DOI: 10.4319/lo.1992.37.7.1447

Holtgrieve GW, Schindler DE, Branch TA, and A'mar ZT. 2010. Simultaneous quantification of aquatic ecosystem metabolism and reaeration using a Bayesian statistical model of oxygen dynamics. Limnology and Oceanography, 55(3): 1047–1063. DOI: 10.4319/lo.2010.55.3.1047

Hood JLA. 2012. The role of submersed macrophytes in river eutrophication and biogeochemical nutrient cycling. Ph.D. thesis, University of Waterloo, Waterloo, Ontario. Available from hdl.handle.net/10012/7084.

Hood JLA, Taylor WD, and Schiff SL. 2014. Examining the fate of WWTP effluent nitrogen using $\delta^{15}N\text{-}NH_4^+$, $\delta^{15}N\text{-}NO_3^-$ and $\delta^{15}N$ of submersed macrophytes. Aquatic Sciences, 76(2): 243–258. DOI: 10.1007/s00027-013-0333-4

Iwanyshyn M, Ryan MC, and Chu A. 2008. Separation of physical loading from photosynthesis/respiration processes in rivers by mass balance. Science of the Total Environment, 390(1): 205–214. PMID: 17976689 DOI: 10.1016/j.scitotenv.2007.09.038

Jähne B, Münnich KO, Bösinger R, Dutzi A, Huber W, and Libner P. 1987. On the parameters influencing air-water gas exchange. Journal of Geophysical Research: Oceans, 92(C2): 1937–1949. DOI: 10.1029/JC092iC02p01937

Jamieson TS, Schiff SL, and Taylor WD. 2013. Using stable isotopes of dissolved oxygen for the determination of gas exchange in the Grand River, Ontario, Canada. Water Research, 47(2): 781–790. PMID: 23206500 DOI: 10.1016/j.watres.2012.11.001

Johnson MT. 2010. A numerical scheme to calculate temperature and salinity dependent air-water transfer velocities for any gas. Ocean Science, 6(4): 913–932. DOI: 10.5194/os-6-913-2010

Karrow PF. 1974. Till stratigraphy in parts of southwestern Ontario. Geological Society of America Bulletin, 85(5): 761. DOI: 10.1130/0016-7606(1974)85<761:TSIPOS>2.0.CO;2

Kirshenbaum I, Smith JS, Crowell T, Graff J, and McKee R. 1947. Separation of the nitrogen isotopes by the exchange reaction between ammonia and solutions of ammonium nitrate. The Journal of Chemical Physics, 15(7): 440–446. DOI: 10.1063/1.1746562

Kreith F. 2000. The CRC handbook of thermal engineering. Springer Science & Business Media, Berlin.

Laursen AE, and Seitzinger SP. 2002. Measurement of denitrification in rivers: an integrated, whole reach approach. Hydrobiologia, 485(1/3): 67–81. DOI: 10.1023/A:1021398431995

Laursen AE, and Seitzinger SP. 2004. Diurnal patterns of denitrification, oxygen consumption and nitrous oxide production in rivers measured at the whole-reach scale. Freshwater Biology, 49(11): 1448–1458. DOI: 10.1111/j.1365-2427.2004.01280.x

Li L, Lollar BS, Li H, Wortmann UG, and Lacrampe-Couloume G. 2012. Ammonium stability and nitrogen isotope fractionations for NH_4^+-$NH_{3(aq)}$-$NH_{3(gas)}$ systems at 20–70°C and pH of 2–13: applications to habitability and nitrogen cycling in low-temperature hydrothermal systems. Geochimica et Cosmochimica Acta, 84: 280–296. DOI: 10.1016/j.gca.2012.01.040

Loomer HA. 2008. The dynamics of carbon and nitrogen stable isotope analysis of aquatic organisms within the Grand River watershed. M.Sc. thesis, University of Waterloo, Waterloo, Ontario [online]: Available from hdl.handle.net/10012/4263.

Loomer HA, Oakes KD, Schiff SL, Taylor WD, and Servos MR. 2014. Use of stable isotopes to trace municipal wastewater effluents into food webs within a highly developed river system. River Research and Applications, 31(9): 1093–1100. DOI: 10.1002/rra.2826

MacIsaac JJ, and Dugdale RC. 1969. The kinetics of nitrate and ammonia uptake by natural populations of marine phytoplankton. Deep Sea Research and Oceanographic Abstracts, 16(1): 45–57. DOI: 10.1016/0011-7471(69)90049-7

Mariotti A, Germon JC, Hubert P, Kaiser P, Letolle R, Tardieux A, et al. 1981. Experimental determination of nitrogen kinetic isotope fractionation: some principles; illustration for the denitrification and nitrification processes. Plant and Soil, 62(3): 413–430. DOI: 10.1007/BF02374138

Mariotti A, Mariotti F, Champigny M-L, Amarger N, and Moyse A. 1982. Nitrogen isotope fractionation associated with nitrate reductase activity and uptake of NO_3^- by pearl millet. Plant Physiology, 69(4): 880–884. PMID: 16662313 DOI: 10.1104/pp.69.4.880

Mészáros E. 1992. Occurrence of atmospheric acidity. *In* Atmospheric acidity: sources, consequences and abatement. *Edited by* M. Radojevic and R.M. Harrison Springer, Berlin. pp. 1–38.

Moore C, and Doherty J. 2005. Role of the calibration process in reducing model predictive error. Water Resources Research, 41(5): W05020. DOI: 10.1029/2004WR003501

Mulholland PJ, Tank JL, Sanzone DM, Wollheim WM, Peterson BJ, Webster JR, et al. 2000. Nitrogen cycling in a forest stream determined by a ^{15}N tracer addition. Ecological Monographs, 70(3): 471–493. DOI: 10.1890/0012-9615(2000)070[0471:NCIAFS]2.0.CO;2

Mulholland PJ, Valett HM, Webster JR, Thomas SA, Cooper LW, Hamilton SK, et al. 2004. Stream denitrification and total nitrate uptake rates measured using a field ^{15}N tracer addition approach. Limnology and Oceanography, 49(3): 809–820. DOI: 10.4319/lo.2004.49.3.0809

Mulholland PJ, Helton AM, Poole GC, Hall RO, Hamilton SK, Peterson BJ, et al. 2008. Stream denitrification across biomes and its response to anthropogenic nitrate loading. Nature, 452(7184): 202–205. PMID: 18337819 DOI: 10.1038/nature06686

Murray M. 2008. Evaluating the isotopic fingerprint of wastewater treatment plant nitrogen and its evolution in the Grand River. B.Sc. thesis, University of Waterloo, Waterloo, Ontario.

Newbold JD, Elwood JW, O'Neill RV, and Winkle WV. 1981. Measuring nutrient spiralling in streams. Canadian Journal of Fisheries and Aquatic Sciences, 38(7): 860–863. DOI: 10.1139/f81-114

Newbold J, O'Neill R, Elwood J, and Van Winkle W. 1982. Nutrient spiralling in streams: implications for nutrient limitation and invertebrate activity. The American Naturalist, 120(5): 628–652. DOI: 10.1086/284017

Newbold JD, Elwood JW, O'Neill RV, and Sheldon AL. 1983. Phosphorus dynamics in a woodland stream ecosystem: a study of nutrient spiralling. Ecology, 64(5): 1249–1265. DOI: 10.2307/1937833

Norlin E, Irgum K, and Ohlsson KEA. 2002. Determination of the $^{15}N/^{14}N$ ratio of ammonium and ammonia in aqueous solutions by equilibrium headspace-gas chromatography-combustion-isotope ratio mass spectrometry. The Analyst, 127(6): 735–740. PMID: 12146904 DOI: 10.1039/b200488g

Olofsson G. 1975. Thermodynamic quantities for the dissociation of the ammonium ion and for the ionization of aqueous ammonia over a wide temperature range. The Journal of Chemical Thermodynamics, 7(6): 507–514. DOI: 10.1016/0021-9614(75)90183-4

Parker SR, Gammons CH, Poulson SR, DeGrandpre MD, Weyer CL, Smith MG, et al. 2010. Diel behavior of stable isotopes of dissolved oxygen and dissolved inorganic carbon in rivers over a range of trophic conditions, and in a mesocosm experiment. Chemical Geology, 269(1–2): 22–32. DOI: 10.1016/j.chemgeo.2009.06.016

Peipoch M, Gacia E, Blesa A, Ribot M, Riera JL, and Martí E. 2014. Contrasts among macrophyte riparian species in their use of stream water nitrate and ammonium: insights from ^{15}N natural abundance. Aquatic Sciences, 76(2): 203–215. DOI: 10.1007/s00027-013-0330-7

Pennock JR, Velinsky DJ, Ludlam JM, Sharp JH, and Fogel ML. 1996. Isotopic fractionation of ammonium and nitrate during uptake by *Skeletonema costatum*: implications for $\delta^{15}N$ dynamics under bloom conditions. Limnology and Oceanography, 41(3): 451–459. DOI: 10.4319/lo.1996.41.3.0451

Petzoldt T, and Rinke K. 2007. simecol: an object-oriented framework for ecological modeling in R. Journal of Statistical Software, 22(9): 1–31. DOI: 10.18637/jss.v022.i09

Posch M, de Smet PAM, Hettelingh JP, and Downing RJ. 2001. Modelling and mapping of critical thresholds in Europe. RIVM Rapport 259101010. Coordination Center for Effects National Institute for Public Health and the Environment, Bilthoven, the Netherlands.

R Core Team. 2016. R: a language and environment for statistical computing. R Foundation for Statistical Computing, Vienna, Austria [online]: Available from R-project.org/.

Raymond PA, Zappa CJ, Butman D, Bott TL, Potter J, Mulholland P, et al. 2012. Scaling the gas transfer velocity and hydraulic geometry in streams and small rivers. Limnology and Oceanography: Fluids and Environments, 2(1): 41–53. DOI: 10.1215/21573689-1597669

Region of Waterloo. 2011. Residential water softener performance study. Testing Report #1. Region of Waterloo, Waterloo, Ontario.

Rosamond MS, Thuss SJ, Schiff SL, and Elgood RJ. 2011. Coupled cycles of dissolved oxygen and nitrous oxide in rivers along a trophic gradient in southern Ontario, Canada. Journal of Environment Quality, 40(1): 256–270. PMID: 21488515 DOI: 10.2134/jeq2010.0009

Rosamond MS, Thuss SJ, and Schiff SL. 2012. Dependence of riverine nitrous oxide emissions on dissolved oxygen levels. Nature Geoscience, 5: 715–718. DOI: 10.1038/ngeo1556

Saloranta TM, Kämäri J, Rekolainen S, and Malve O. 2003. Benchmark criteria: a tool for selecting appropriate models in the field of water management. Environmental Management, 32(3): 322–333. PMID: 14753618 DOI: 10.1007/s00267-003-0069-3

Savage C, and Elmgren R. 2004. Macroalgal (*Fucus vesiculosus*) $\delta^{15}N$ values trace decrease in sewage influence. Ecological Applications, 14(2): 517–526. DOI: 10.1890/02-5396

Schindler DW. 1998. Whole-ecosystem experiments: replication versus realism: the need for ecosystem-scale experiments. Ecosystems, 1(4): 323–334. DOI: 10.1007/s100219900026

Schindler DW, Dillon PJ, and Schreier H. 2006. A review of anthropogenic sources of nitrogen and their effects on Canadian aquatic ecosystems. Biogeochemistry, 79(1–2): 25–44. DOI: 10.1007/s10533-006-9001-2

Sebilo M, Billen G, Grably M, and Mariotti A. 2003. Isotopic composition of nitrate-nitrogen as a marker of riparian and benthic denitrification at the scale of the whole Seine River system. Biogeochemistry, 63(1): 35–51. DOI: 10.1023/A:1023362923881

Sharpley AN, Kleinman PJA, Jordan P, Bergström L, and Allen AL. 2009. Evaluating the success of phosphorus management from field to watershed. Journal of Environment Quality, 38(5): 1981–1988. PMID: 19704141 DOI: 10.2134/jeq2008.0056

Snider DM, Spoelstra J, Schiff SL, and Venkiteswaran JJ. 2010. Stable oxygen isotope ratios of nitrate produced from nitrification: ^{18}O-labeled water incubations of agricultural and temperate forest soils. Environmental Science and Technology, 44(14): 5358–5364. PMID: 20550183 DOI: 10.1021/es1002567

Snider DM, Venkiteswaran JJ, Schiff SL, and Spoelstra J. 2012. Deciphering the oxygen isotope composition of nitrous oxide produced by nitrification. Global Change Biology, 18(1): 356–370. DOI: 10.1111/j.1365-2486.2011.02547.x

Snider DM, Venkiteswaran JJ, Schiff SL, and Spoelstra J. 2013. A new mechanistic model of $\delta^{18}O$-N_2O formation by denitrification. Geochimica et Cosmochimica Acta, 112: 102–115. DOI: 10.1016/j.gca.2013.03.003

Snider DM, Venkiteswaran JJ, Schiff SL, and Spoelstra J. 2015. From the ground up: global nitrous oxide sources are constrained by stable isotope values. PLoS ONE, 10(3): e0118954. PMID: 25811179 DOI: 10.1371/journal.pone.0118954

Spoelstra J. 2004. Nitrate sources and cycling at the Turkey Lakes Watershed: a stable isotope approach. Ph.D. thesis, University of Waterloo, Waterloo, Ontario [online]: Available from hdl.handle.net/10012/1240.

Tank JL, Meyer JL, Sanzone DM, Mulholland PJ, Webster JR, Peterson BJ, et al. 2000. Analysis of nitrogen cycling in a forest stream during autumn using a ^{15}N-tracer addition. Limnology and Oceanography, 45(5): 1013–1029. DOI: 10.4319/lo.2000.45.5.1013

Thode HG, Graham RL, and Ziegler JA. 1945. A mass spectrometer and the measurement of isotope exchange factors. Canadian Journal of Research, 23b(1): 40–47. DOI: 10.1139/cjr45b-006

Thuss SJ, Venkiteswaran JJ, and Schiff SL. 2014. Proper interpretation of dissolved nitrous oxide isotopes, production pathways, and emissions requires a modelling approach. PLoS ONE, 9(3): e90641. PMID: 24608915 DOI: 10.1371/journal.pone.0090641

Tobias CR, Böhlke JK, and Harvey JW. 2007. The oxygen-18 isotope approach for measuring aquatic metabolism in high productivity waters. Limnology and Oceanography, 52(4): 1439–1453. DOI: 10.4319/lo.2007.52.4.1439

van Kessel MA, Speth DR, Albertsen M, Nielsen PH, Op den Camp HJ, Kartal B, et al. 2015. Complete nitrification by a single microorganism. Nature, 528: 555–559. PMID: 26610025 DOI: 10.1038/nature16459

Veale B, and Cooke S. 2016. Implementing integrated water management: illustrations from the Grand River watershed. International Journal of Water Resources Development, 33: 375–392. DOI: 10.1080/07900627.2016.1217503

Venkiteswaran JJ, Wassenaar LI, and Schiff SL. 2007. Dynamics of dissolved oxygen isotopic ratios: a transient model to quantify primary production, community respiration, and air–water exchange in aquatic ecosystems. Oecologia, 153(2): 385–398. PMID: 17516090 DOI: 10.1007/s00442-007-0744-9

Venkiteswaran JJ, Rosamond MS, and Schiff SL. 2014. Nonlinear response of riverine N_2O fluxes to oxygen and temperature. Environmental Science and Technology, 48(3): 1566–1573. PMID: 24410177 DOI: 10.1021/es500069j

Venkiteswaran JJ, Schiff SL, and Taylor WD. 2015. Linking aquatic metabolism, gas exchange, and hypoxia to impacts along the 300-km Grand River, Canada. Freshwater Science, 34(4): 1216–1232. DOI: 10.1086/683241

Wassenaar LI, Venkiteswaran JJ, Schiff SL, and Koehler G. 2010. Aquatic community metabolism response to municipal effluent inputs in rivers quantified using diel $\delta^{18}O$ values of dissolved oxygen. Canadian Journal of Fisheries and Aquatic Sciences, 67(8): 1232–1246. DOI: 10.1139/F10-057

Webster JR, Mulholland PJ, Tank JL, Valett HM, Dodds WK, Peterson BJ, et al. 2003. Factors affecting ammonium uptake in streams—an inter-biome perspective. Freshwater Biology, 48(8): 1329–1352. DOI: 10.1046/j.1365-2427.2003.01094.x

Withers PJ, and Lord EI. 2002. Agricultural nutrient inputs to rivers and groundwaters in the UK: policy, environmental management and research needs. Science of the Total Environment, 282–283: 9–24. PMID: 11852908 DOI: 10.1016/S0048-9697(01)00935-4

Yoneyama T, Omata T, Nakata S, and Yazaki J. 1991. Fractionation of nitrogen isotopes during the uptake and assimilation of ammonia by plants. Plant and Cell Physiology, 32(8): 1211–1217. DOI: 10.1093/oxfordjournals.pcp.a078199

Yoneyama T, Fujihara S, and Yagi K. 1998. Natural abundance of ^{15}N in amino acids and polyamines from leguminous nodules: unique ^{15}N enrichment in homospermidine. Journal of Experimental Botany, 49(320): 521–526. DOI: 10.1093/jxb/49.320.521

Yoneyama T, Matsumaru T, Usui K, and Engelaar WMHG. 2001. Discrimination of nitrogen isotopes during absorption of ammonium and nitrate at different nitrogen concentrations by rice (*Oryza sativa* L.) plants. Plant, Cell and Environment, 24(1): 133–139. DOI: 10.1046/j.1365-3040.2001.00663.x

Zhang L, Altabet MA, Wu T, and Hadas O. 2007. Sensitive measurement of NH_4^+ $^{15}N/^{14}N$ ($\delta^{15}NH_4^+$) at natural abundance levels in fresh and saltwaters. Analytical Chemistry, 79(14): 5297–5303. PMID: 17567102 DOI: 10.1021/ac070106d